FINITE DIFFERENCE METHODS FOR COUPLED FLOW INTERACTION TRANSPORT MODELS

SHELLY MCGEE, PADMANABHAN SESHAIYER

ABSTRACT. Understanding chemical transport in blood flow involves coupling the chemical transport process with flow equations describing the blood and plasma in the membrane wall. In this work, we consider a coupled two-dimensional model with transient Navier-Stokes equation to model the blood flow in the vessel and Darcy's flow to model the plasma flow through the vessel wall. The advection-diffusion equation is coupled with the velocities from the flows in the vessel and wall, respectively to model the transport of the chemical. The coupled chemical transport equations are discretized by the finite difference method and the resulting system is solved using the additive Schwarz method. Development of the model and related analytical and numerical results are presented in this work.

1. INTRODUCTION

Mathematical modelling of blood flow in the small vessels is a challenging problem and has been of great interest to many researchers. This problem coupled with models for the transport of chemicals in the blood stream brings new challenges in the solution methodology. In this paper, we present and analyze a model that couples blood flow and chemical transport where a discontinuous solution in the chemical concentration along one boundary is allowed.

Specifically, we consider a mathematical model for coupling blood flow and chemical transport in the arteries. The Navier-Stokes equation in two-dimensions is used to model the blood flow in an artery and Darcy's flow is used to model the plasma flow through the arterial wall. These respective flow equations are coupled at the arterial wall boundary through appropriate interface conditions. For the chemical transport model, the advection-diffusion equation is employed both inside the artery and the arterial wall, and the velocities are coupled at the arterial wall. The coupled model is discretized via the finite difference method. In particular, we employ an explicit finite difference method for the blood flow and an implicit finite difference method for the advection-diffusion equation. Note that it is also

important to take into account that the concentration across the boundary from the vessel to the wall does not have to be continuous; we employ an iterative Schwarz type algorithm to accomplish this.

2. Background, models, and methods

In this section, we will describe the models that are employed for the blood flow, plasma flow and chemical transport on a two dimensional domain (figure 1.)
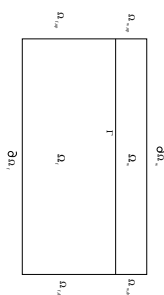

FIGURE 1. The domain partitioned into the two domains Ω_f and Ω_w.

Consider figure 1, where the geometry is partitioned into two subdomains, Ω_f and Ω_w, where Ω_f denotes the domain for the blood flow and Ω_w denotes the domain for the flow of plasma in the vessel wall. The interface between Ω_f and Ω_w is Γ, where the two velocities are coupled as well as the chemical concentrations from the respective advection-diffusion equatons. Next, we describe the equations in the respective subdomains.

2.1. **Model for blood flow.** The Navier-Stokes Equation in two-dimensions that is employed to model the blood flow can be expressed as

$$\rho\frac{\partial \mathbf{u}}{\partial t} + \rho(\mathbf{u}\cdot\nabla)\mathbf{u} - \nu\Delta\mathbf{u} + \nabla p = \mathbf{f} \tag{2.1}$$

$$\nabla\cdot\mathbf{u} = 0. \tag{2.2}$$

where $\mathbf{u} = \mathbf{u}(\mathbf{x},t) = (u(x,y,t),v(x,y,t))^T$ where $u(x,y,t)$ (cm/sec) is the velocity in the x direction at the point (x,y) at time t and $v(x,y,t)$ (cm/sec) is the velocity in the y direction at the point (x,y) at time t, ρ is the density of the fluid (g/cm^3), ν is the viscosity of the fluid (g/(cm$^2\cdot$ sec)), $p = p(x,y,t)$ is the pressure at the point (x,y) at time t (g/(cm·sec^2)), and $\mathbf{f}$ is any external forces acting on the fluid at point (x,y) at time t (g/(cm^{2}sec^2)). Equation (2.1) is called the *momentum equation* and is derived from the conservation of momentum which describes the motion of the particles in the fluid. Equation (2.2) is called the *continuity equation* which is derived from the conservation of mass.

Note that (2.1)-(2.2) can be written in component form as

$$\rho\frac{\partial u}{\partial t} + \rho\Big(\frac{\partial(u^2)}{\partial x} + \frac{\partial(uv)}{\partial y}\Big) - \nu\Big(\frac{\partial^2 u}{\partial x^2} + \frac{\partial^2 u}{\partial y^2}\Big) + \frac{\partial p}{\partial x} = f_1 \tag{2.3}$$

$$\rho\frac{\partial v}{\partial t} + \rho\left(\frac{\partial(uv)}{\partial x} + \frac{\partial(v^2)}{\partial y}\right) - \nu\left(\frac{\partial^2 v}{\partial x^2} + \frac{\partial^2 v}{\partial y^2}\right) + \frac{\partial p}{\partial y} = f_2 \tag{2.4}$$

$$\frac{\partial u}{\partial x} + \frac{\partial v}{\partial y} = 0 \tag{2.5}$$

where $\mathbf{f} = (f_1(x,y,t), f_2(x,y,t))^T$.

We solve (2.3)-(2.5) on Ω_f with boundary conditions

$$\mathbf{u} = u_{\text{in}}(0,y,t) = U(t)(R^2 - y^2) \quad \text{on } \Omega_{f,up} \tag{2.6}$$

$$\frac{\partial \mathbf{u}}{\partial x} = 0 \quad \text{on } \Omega_{f,dw} \tag{2.7}$$

$$v(x,0) = 0 \quad \text{on } \partial\Omega_f \tag{2.8}$$

$$\frac{\partial u(0,x)}{\partial y} = 0 \quad \text{on } \partial\Omega_f \tag{2.9}$$

$$\mathbf{u} = 0 \quad \text{on } \Gamma \tag{2.10}$$

where $u_{in}(0,y,t)$ is the prescribed inflow velocity upstream on $\Omega_{f,up}$, R is the width of the domain in the y direction, and $U(t) = (1 - \cos((2\pi t + \pi)/T_p))/2$ or $U(t)$ is a constant depending on whether the inflow is time varying or constant [2, 3, 7]. T_p is the pulse period. Equation (2.6) is the inflow boundary condition, and (2.7) is the outflow boundary condition downstream. Equations (2.8) and (2.9) are free slip boundary conditions. These boundary conditions allow the original domain to be cut in half during the computations since the flow will be symmetric about $\partial\Omega_f$. Equation (2.10) is the no slip boundary condition. An initial condition $\mathbf{u}(\mathbf{x},0)$ is also prescribed along with the boundary conditions.

2.2. Model for plasma flow. Since the blood vessel wall is porous as in saturated ground water flow, we employ Darcy's Law to describe the flow of plasma through the vessel wall [3]. This is written as

$$\mathbf{u}_{\text{filt}} = -K\nabla p \tag{2.11}$$

$$\nabla \cdot \mathbf{u}_{\text{filt}} = 0 \tag{2.12}$$

where $\mathbf{u}_{\text{filt}}$ is the filtration velocity of the fluid (cm/sec), K is the conductivity of the porous media (cm^{3}sec/g), and p is the pressure. Equation (2.12) can be interpreted as the filtration velocity is equal over the domain. This is a result of the porous media being saturated. Applying the gradient operator to (2.11), the equation becomes [3]

$$\nabla \cdot \mathbf{u}_{\text{filt}} = \nabla \cdot (K\nabla p) \tag{2.13}$$

which yields

$$0 = \Delta p, \tag{2.14}$$

if K is considered to be a constant. Equation (2.14) is solved on Ω_w with the boundary conditions given by

$$p = p_0(\mathbf{x}) \quad \text{on } \Gamma \tag{2.15}$$

$$p = p_1(\mathbf{x}) \quad \text{on } \partial\Omega_w \tag{2.16}$$

$$\frac{\partial p}{\partial \mathbf{n}} = 0 \quad \text{on } \partial\Omega_{w,up} \text{ and } \partial\Omega_{w,dw} \tag{2.17}$$

and then use the solution p in (2.11) to solve $\mathbf{u}_{\text{filt}}$ for a known K.

2.3. **Chemical transport in blood flow.** The chemical transport for a flow system such as blood flow is modelled by the advection-diffusion equation

$$\frac{\partial C}{\partial t} - D\Delta C + \mathbf{u} \cdot \nabla C = s \tag{2.18}$$

with appropriate boundary conditions where C is the concentration at (x,y) in (g/cm^3), D is the diffusivity in (cm^2/sec), $\mathbf{u}$ is the velocity of the fluid in (cm/sec), and s is a source term in $(g/(cm^3 sec))$. For the flow structure system described previously, two advection-diffusion equations are needed, one to describe concentration C_f in the fluid domain, Ω_f, and the other for the concentration C_w in the structure domain, Ω_w. Since the interface Γ represents a physical barrier that is a selectively permeable membrane (the blood vessel wall) the concentrations C_f and C_w do not have to match at Γ (see figure 1). The rate at which the chemical crosses the membrane is proportional to the gradient between the two concentrations at the barrier Γ [7]. The resulting system then becomes:

$$\frac{\partial C_f}{\partial t} - D_f \Delta C_f + \mathbf{u}_f \cdot \nabla C_f = s_f \text{ in } \Omega_f$$
$$\frac{\partial C_w}{\partial t} - D_w \Delta C_w + \mathbf{u}_w \cdot \nabla C_w = s_w \text{ in } \Omega_w \tag{2.19}$$

with boundary conditions

$$D_f \frac{\partial C_f}{\partial y} + \zeta(C_f - C_w) = 0 \quad \text{on } \Gamma \tag{2.20}$$

$$D_w \frac{\partial C_w}{\partial y} + \zeta(C_w - C_f) = 0 \quad \text{on } \Gamma \tag{2.21}$$

$$C_f = C_0 \quad \text{on } \partial\Omega_{f,up} \tag{2.22}$$

$$D_f \frac{\partial C_f}{\partial x} = 0 \quad \text{on } \partial\Omega_{f,dw} \tag{2.23}$$

$$C_w = C_0 \quad \text{on } \partial\Omega_{w,up} \tag{2.24}$$

$$D_w \frac{\partial C_w}{\partial x} = 0 \quad \text{on } \partial\Omega_{w,dw}, \tag{2.25}$$

where D_f is the diffusivity in Ω_f, D_w is the diffusivity in Ω_w, ζ is the permeability of the membrane that Γ represents, and is calculated from a function of the shear stress $\tilde{\sigma}$ exerted by the blood on the wall. Initial conditions are $C_f = C_{f0}$ and $C_w = C_{w0}$ at $t = 0$.

Remark 2.1. The boundary conditions in (2.20) and (2.21), when added together yield

$$D_f \frac{\partial C_f}{\partial y} = -D_w \frac{\partial C_w}{\partial y}, \tag{2.26}$$

which says that the flux out of Ω_f is equal to the flux into Ω_w, and indeed this makes sense physically.

3. Finite Difference Methods

Next, we describe the discretized equations for the respective models using the finite difference methods. First, we will present the details of the discretization and implementation for the flow equations. Then we will present the discretization of the advection-diffusion equation and details for implementing the discontinuity in the concetrations at the arterial wall via an Addivite Schwarz type iterative method.

3.1. Discretization of the flow equations.
In this work, an explicit finite difference method [2, 5] is employed to solve the Navier-Stokes equation. The discretized system for (2.3)-(2.4) becomes

$$\frac{u^{n+1} - u^n}{\Delta t} = \frac{\nu}{\rho}\left(\frac{\partial^2 u^n}{\partial x^2} + \frac{\partial^2 u^n}{\partial y^2}\right) - \left(\frac{\partial((u^n)^2)}{\partial x} + \frac{\partial(uv)^n}{\partial y}\right) - \frac{1}{\rho}\frac{\partial p^{n+1}}{\partial x} + g_1^n, \quad (3.1)$$

$$\frac{v^{n+1} - v^n}{\Delta t} = \frac{\nu}{\rho}\left(\frac{\partial^2 v^n}{\partial x^2} + \frac{\partial^2 v^n}{\partial y^2}\right) - \left(\frac{\partial(uv)^n}{\partial x} + \frac{\partial((v^n)^2)}{\partial y}\right) - \frac{1}{\rho}\frac{\partial p^{n+1}}{\partial y} + g_2^n, \quad (3.2)$$

where $g_1^n = \frac{1}{\rho}f_1(u^n, v^n, t_n)$ and $g_2 = \frac{1}{\rho}f_2(u^n, v^n, t_n)$. Here $u^n = u(\mathbf{x}, t_n)$, $v^n = v(\mathbf{x}, t_n)$, $t_n = t_0 + n\Delta t$, t_0 is the initial time, n is the number of time steps from the initial time to t_n, and Δt is the size of the time step. Solving (3.1) for u^{n+1} and (3.2) for v^{n+1} gives the equations

$$u^{n+1} = F^n - \Delta t \frac{1}{\rho}\frac{\partial p^{n+1}}{\partial x}, \quad (3.3)$$

$$v^{n+1} = G^n - \Delta t \frac{1}{\rho}\frac{\partial p^{n+1}}{\partial y} \quad (3.4)$$

where

$$\begin{aligned} F^n &= F(u^n, v^n, t_n) \\ &= u^n + \Delta t\left[\frac{\nu}{\rho}\left(\frac{\partial^2 u^n}{\partial x^2} + \frac{\partial^2 u^n}{\partial y^2}\right) - \left(\frac{\partial((u^n)^2)}{\partial x} + \frac{\partial(u^n v^n)}{\partial y}\right) + g_1^n\right], \end{aligned} \quad (3.5)$$

and

$$\begin{aligned} G^n &= G(u^n, v^n, t_n) \\ &= v^n + \Delta t\left[\frac{\nu}{\rho}\left(\frac{\partial^2 v^n}{\partial x^2} + \frac{\partial^2 v^n}{\partial y^2}\right) - \left(\frac{\partial(u^n v^n)}{\partial x} + \frac{\partial((v^n)^2)}{\partial y}\right) + g_2^n\right]. \end{aligned} \quad (3.6)$$

Substituting u^{n+1} and v^{n+1} from (3.3)-(3.4) into the discretized continuity equation (2.5) we get

$$\frac{\partial u^{n+1}}{\partial x} + \frac{\partial v^{n+1}}{\partial y} = \frac{\partial F^n}{\partial x} - \frac{\Delta t}{\rho}\frac{\partial^2 p^{n+1}}{\partial x^2} + \frac{\partial G^n}{\partial y} - \frac{\Delta t}{\rho}\frac{\partial^2 p^{n+1}}{\partial y^2} = 0 \quad (3.7)$$

which reduces to

$$\frac{\partial^2 p^{n+1}}{\partial x^2} + \frac{\partial^2 p^{n+1}}{\partial y^2} = \frac{\rho}{\Delta t}\left((\frac{\partial F^n}{\partial x} + \frac{\partial G^n}{\partial y}\right). \quad (3.8)$$

Since an initial condition is required, $u(x, y, 0) = u^0$, $v(x, y, 0) = v^0$, and $p(x, y, 0) = p^0$ are known, hence F^0 and G^0 can be calculated. Thus, the right hand side of
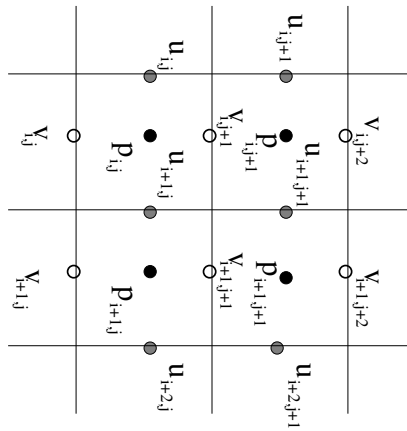
FIGURE 2. Staggered grid for the Navier-Stokes discretization.

(3.8) is known, and p^{n+1} can be calculated. Using (3.3)-(3.4) one can then compute u^{n+1} and v^{n+1}.

Now the spatial derivatives are discretized also using finite differences. Central differences are used to approximate first derivative terms $\frac{\partial p^{n+1}}{\partial x}$, $\frac{\partial p^{n+1}}{\partial y}$, $\frac{\partial F^n}{\partial x}$, and $\frac{\partial G^n}{\partial y}$. A staggered grid, shown in figure 2, is used to calculate u and v because oscillations can occur in grids where u and v are calculated at the same point [2]. Bilinear interpolation is used to calculate u, v, and p at points other than node points [6]. Notice that $\frac{\partial p^{n+1}}{\partial x}$ is used in (3.3) to calculate $u(x_i, y_{j+1/2}, t_{n+1})$, where $x_i = x_0 + i\Delta x$, $i = 0, 1, 2, \ldots, I$, and $y_{j+1/2} = y_0 + (j + 1/2)\Delta y$, $j = 0, 1, 2, \ldots, J$, x_0 and y_0 are the smallest values in the domain, Δx and Δy are the step sizes in the x and y direction, respectively, and I and J are the number of steps in the x and y directions, respectively, and must be integers. The half steps are due to the staggered grid (see figure 2). Let us use the notation $u_{i,j}^n = u(x_i, y_{j+1/2}, t_n)$ and $u_{i+1,j}^n = u(x_{i+1}, y_{j+1/2}, t_n)$ from now on. Simple central differences on convection terms can cause oscillations in the numerical solution that are not physically occurring [2, 5]. The solution methodology used here employs a donor-cell scheme.

Now the boundary conditions in (2.6)-(2.10) for the staggered grid will be formulated as follows. The inflow condition given in (2.6) for the velocity in the x direction is

$$u_{i,j}^n = U(t_n)(R^2 - y_{j+1/2}^2), \quad \text{for } i = 0 \text{ and } j = 1, \ldots, J. \tag{3.9}$$

The inflow in the y direction is zero so

$$v(0, y, t) = 0,$$

but since v is evaluated at the points $(x_{-1/2}, y_j, t_n)$ and $(x_{1/2}, y_j, t_n)$, v on the boundary is calculated by

$$v(0, y_j, t) = v(x_{-1/2}, y_j, t_n) + v(x_{1/2}, y_j, t_n) = 0$$

leading to the boundary condition for the method formulated as

$$v_{i,j}^n = -v_{i+1,j}^n \quad \text{for } i = 0 \text{ and } j = 0, \ldots, J,$$

using the numbering scheme shown on the grid in figure 2. The outflow condition given in (2.7) is

$$u_{i,j}^n = u_{i-1,j}^n \quad \text{for } i = I \text{ and } j = 0, \ldots, J+1,$$

and

$$v_{i,j}^n = v_{i-1,j}^n \quad \text{for } i = I+1 \text{ and } j = 0, \ldots, J.$$

The no slip and free slip boundary conditions on the remaining two sides, Γ and $\partial\Omega_f$, respectively, (see figure 1) are

$$u_{i,j}^n = -u_{i,j-1}^n \quad \text{for } i = 0, \ldots, I \text{ and } j = J+1, \tag{3.10}$$

$$v_{i,j}^n = 0 \quad \text{for } i = 0, \ldots, I+1 \text{ and } j = J, \tag{3.11}$$

$$u_{i,j}^n = -u_{i,j+1}^n \quad \text{for } i = 0, \ldots, I \text{ and } j = 0, \tag{3.12}$$

$$v_{i,j}^n = 0 \quad \text{for } i = 0, \ldots, I+1 \text{ and } j = 0. \tag{3.13}$$

Solving the system starts with the initial condition for u, v, and p, supplied by the user. Since this is an explicit finite difference scheme, stability conditions must be met. These conditions can be derived to be

$$\frac{2\nu\Delta t}{\rho} < \Big(\frac{1}{\Delta x^2} + \frac{1}{\Delta y^2}\Big)^{-1}$$

$$|u_{\max}|\Delta t < \Delta x$$

$$|v_{\max}|\Delta t < \Delta y,$$

where $u_{\max} = \max|u_{i,j}^n|$ and $v_{\max} = \max|v_{i,j}^n|$. The last two conditions are the Courant-Friedrichs-Lewy (CFL) conditions and they guarantee that no fluid particle will travel more than Δx or Δy in a single time step Δt. To ensure that all the stability conditions are met, Δt should be chosen so that

$$\Delta t < \min\Big(\frac{\rho}{2\nu}\Big(\frac{1}{\Delta x^2} + \frac{1}{\Delta y^2}\Big)^{-1}, \frac{\Delta x}{|u_{\max}|}, \frac{\Delta y}{|v_{\max}|}\Big). \tag{3.14}$$

After checking the stability condition and adjusting Δt if needed, F^0 and G^0 are calculated from u^0 and v^0. The parameter γ should be chosen as [2]

$$\gamma = \max_{i,j}\Big(\Big|\frac{u_{i,j}^n\Delta t}{\Delta x}\Big|, \Big|\frac{v_{i,j}^n\Delta t}{\Delta y}\Big|\Big) \tag{3.15}$$

Using F^0 and G^0, equation (3.8) is solved using the iterative method, *successive over-relaxation* (SOR). The latter is used because the operations can be performed cell wise without ever having to creating a matrix, but other methods to solve this Poisson equation can also be used. The boundary conditions on p are no flux boundary conditions except at the downstream boundary $\Omega_{f,dn}$, which has a Dirichlet boundary condition in order to avoid problems with uniqueness. Now p^{n+1} is used in equations (3.3) and (3.4) to calculate u and v for the next time step. Then all the boundary conditions are updated and the processes is repeated.

On Ω_w (see figure 1) the equation for the pressure $\Delta p = 0$ or

$$\frac{\partial^2 p}{\partial x^2} + \frac{\partial^2 p}{\partial y^2} = 0 \tag{3.16}$$

is solved for p with Dirichlet boundary conditions on the upper and lower boundaries and no flux boundary conditions on the sides. Using a finite difference discretization via central differences this equation can be transformed into a matrix system that

can be solved using several efficient matrix solver routines. Then p is used to solve for u and v with

$$u = -K\frac{\partial p}{\partial x}, \tag{3.17}$$

$$v = -K\frac{\partial p}{\partial y}, \tag{3.18}$$

where $\frac{\partial p}{\partial x}$ and $\frac{\partial p}{\partial y}$ use central differences for first order derivatives.

Remark 3.1. In the coupled system consisting of Ω_f and Ω_w shown in figure 1, matching flow velocities and pressure at the interface Γ is required. This is accomplished by using the pressure at Γ from Ω_f as the boundary condition at Γ on Ω_w. Then after u and v are calculated for Ω_w, u and v at Γ are used for the boundary conditions at Γ in Ω_f as

$$u_{i,j}^n = u_{w\ i,0}^n \Delta x_f - u_{i,j-1}^n \quad \text{for } i = 0, \dots, I \text{ and } j = J+1, \tag{3.19}$$

$$v_{i,j}^n = v_{w\ i,0}^n \quad \text{for } i = 0, \dots, I+1 \text{ and} j = J, \tag{3.20}$$

where $u_{w\ i,0}$ and $v_{w\ i,0}$ is velocity from Ω_w (which may be interpolated values if the grids are non-matching) and Δx_f is the step size in the x direction on Ω_f.

3.2. **Discretization of the coupled problem.** The time discretized system for the advection-diffusion equation system (2.19)-(2.25) can be written using an implicit scheme in time and employing an additive Schwarz technique [8] as:

$$C_f^{n+1,k+1} + \Delta t \mathcal{L}_f(C_f^{n+1,k+1}) = \Delta t s_f^{n+1,k+1} + C_f^n \tag{3.21}$$

$$C_w^{n+1,k+1} + \Delta t \mathcal{L}_w(C_w^{n+1,k+1}) = \Delta t s_w^{n+1,k+1} + C_w^n \tag{3.22}$$

$$D_f \frac{\partial C_f^{n+1,k+1}}{\partial y} + \zeta C_f^{n+1,k+1} = \zeta C_w^{n+1,k} \tag{3.23}$$

$$D_w \frac{\partial C_w^{n+1,k+1}}{\partial y} + \zeta C_w^{n+1,k+1} = \zeta C_f^{n+1,k} \tag{3.24}$$

$$\mathcal{B}_f(C_f^{n+1,k+1}) = g_f^{n+1,k+1} \tag{3.25}$$

$$\mathcal{B}_w(C_w^{n+1,k+1}) = g_w^{n+1,k+1} \tag{3.26}$$

where n and $n+1$ are the time steps, and k and $k+1$ are the iteration number. C_f^n and C_w^n are known from the previous time step, $C_f^{n+1,k}$ and $C_w^{n+1,k}$ are known from the previous iteration, and $C_f^{n+1,k+1}$ and $C_w^{n+1,k+1}$ are the unknown values for which the system will be solved. $\mathcal{B}_f$ and $\mathcal{B}_w$ are the boundary functions for the boundaries of Ω_f and Ω_w, respectively. They do not contain information about the interface Γ shared by both domains.

Remark 3.2. The additive Schwarz method is a domain decomposition method that allows the problem on each domain to be solved independently, then the values common to both domains are exchanged and the solution is calculated again. This is repeated until the change in the solution in successive iterations is smaller than a user supplied tolerance [8]. The additive Schwarz method can have a region of overlap that in two dimensions has a positive area. In these cases the solution on the two domains is continuous, and in fact, the two domains could quite naturally be computed as a single domain, but are divided to solve each domain simultaneously

on separate processors. In the case discussed here, the overlap is only the interface Γ.

Applying discretizations, the above system can be written in the matrix form

$$A_1 C_f^{n+1,k+1} = f_1^{n+1,k+1} + B_1 C_w^{n+1,k}$$
$$A_2 C_w^{n+1,k+1} = f_2^{n+1,k+1} + B_2 C_f^{n+1,k}$$

where $f_1^{n+1,k+1} = s_f^{n+1,k+1} + C_f^n$, A_1 is the matrix associated Ω_f and the boundaries of Ω_f, B_1 is associated with the interface Γ on the Ω_f side, and the second equation is analogous for Ω_w.

Remark 3.3. One can check that that finite difference scheme presented for the coupled problem is consistent and stable [4]. One can also derive the following error estimate: The l_∞ error for the two domain system (3.21)-(3.26) can be shown to be [4]

$$E_f^{n+1} + E_w^{n+1} \leq n\Delta t \frac{\bar{K}}{1 - \hat{K}} (T_f + T_w) \tag{3.27}$$

where

$$E_f^{n+1} = \max_{i,j \in \Omega_f} |C_{f_{i,j}}^{n+1} - C_f(x_i, y_j, t_{n+1})|$$
$$E_w^{n+1} = \max_{i,j \in \Omega_w} |C_{w_{i,j}}^{n+1} - C_w(x_i, y_j, t_{n+1})|$$

are the respective errors between the exact solution and the finite difference solution at the time level t_{n+1} and T_f and T_w are the respective truncation errors in the fluid and the wall respectively. One can show that [4], as Δt, Δx, and Δy go to zero, $\bar{K}$ goes to one and $\hat{K}$ goes to zero, so that the coefficient in front of the truncation errors is going to one, and as the truncation errors go the zero the method is convergent. The details of the proof can be found in [4].

4. NUMERICAL RESULTS AND DISCUSSION

In this section, we present numerical experiments that models the methods developed in earlier sections. The method is validated by employing exact solutions to known boundary conditions and evaluating the magnitude of the truncation errors. Several exact solutions are tested and the calculated finite difference solution is compared with the exact solution. It is shown that the error in the method is less than the truncation error.

Consider the exact solutions

$$C_f(x, y, t) = -tx(2 - x)y^2 \quad \text{on } 0 \leq x \leq 1, \ 0 \leq y \leq 1$$
$$C_w(x, y, t) = tx(2 - x)y(4 - y) \quad \text{on } 0 \leq x \leq 1, \ 1 \leq y \leq 2$$

that satisfy the advection-diffusion equation

$$\frac{\partial C}{\partial t} = D\left(\frac{\partial^2 C}{\partial x^2} + \frac{\partial^2 C}{\partial y^2}\right) - u\frac{\partial C}{\partial x} - v\frac{\partial C}{\partial y} + f \tag{4.1}$$

where f is a source term. Here, D, u, and v are all set to one (for simplicity), and the source term on Ω_f can be calculated as

$$f_f = -2ty^2 + 2tx(2 - x) - t(2 - 2x)y^2 - 2tx(2 - x)y - x(2 - x)y^2, \tag{4.2}$$

and the source term on Ω_w can be calculated as

$$f_w = 2ty(4-y)+2tx(2-x)+t(2-2x)y(4-y)+tx(2-x)(4-2y)+x(2-x)y(4-y). \tag{4.3}$$

The boundary conditions for C_f are given by

$$C_f(0,y,t) = 0 \tag{4.4}$$

$$\frac{\partial C_f(1,y,t)}{\partial x} = 0 \tag{4.5}$$

$$\frac{\partial C_f(x,0,t)}{\partial y} = 0 \tag{4.6}$$

$$\frac{\partial C_f(x,1,t)}{\partial y} + \zeta C_f(x,1,t) = \zeta C_w(x,1,t) \tag{4.7}$$

with the initial condition

$$C_f(x,y,0) = 0,$$

and the boundary conditions for C_w are given by

$$C_w(0,y,t) = 0$$

$$\frac{\partial C_w(1,y,t)}{\partial x} = 0$$

$$\frac{\partial C_w(x,2,t)}{\partial y} = 0$$

$$\frac{\partial C_w(x,1,t)}{\partial y} + \zeta C_w(x,1,t) = \zeta C_f(x,1,t)$$

with the initial condition

$$C_w(x,y,0) = 0. \tag{4.8}$$

To satisfy the boundary conditions for C_f and C_w on $y=1$, the function ζ is chosen as $\zeta = -1/2$. One can show that the truncation error for the advection-diffusion equation is bounded as [4]

$$|\tau| \le \left| C_{xxxx}\frac{\Delta x^2}{12} + C_{xxx}\frac{\Delta x^2}{6} + C_{yyyy}\frac{\Delta y^2}{12} + C_{yyy}\frac{\Delta y^2}{6} + C_{tt}\frac{\Delta t}{2} \right|. \tag{4.9}$$

For the exact solution considered, the truncation error is zero. One therefore expects that the difference between the exact and calculated solution will be small enough to attribute to round off error. After setting the code parameters to those values specified above, the maximum absolute error between the exact solution and the calculated solution was found to be 5.5022×10^{-11}, which is indeed small enough to attribute to round off error.

Next, we consider the exact solution

$$C_f(x,y,t) = -t^2 x(2-x)y^2 \quad \text{on } 0 \le x \le 1,\ 0 \le y \le 1$$

$$C_w(x,y,t) = t^2 x(2-x)y(4-y) \quad \text{on } 0 \le x \le 1,\ 1 \le y \le 2,$$

with the boundary and initial conditions shown in (4.4)-(4.8). The parameters D, u, and v are one, and $\zeta = -1/2$. The source term f_f in Ω_f is

$$f_f = -2t^2 y^2 + 2t^2 x(2-x) - t^2(2-2x)y^2 - 2t^2 x(2-x)y - 2tx(2-x)y^2 \tag{4.10}$$

and the source term in Ω_w is

$$f_w = 2t^2 y(4-y)+2t^2 x(2-x)+t^2(2-2x)y(4-y)+t^2 x(2-x)(4-2y)+2tx(2-x)y(4-y).$$

n	Δt	$\max\lvert C - C_{\text{exact}}\rvert$	T
1	1	.8224	5
10	.1	.0988	.5
100	.01	.0100	.05
1000	.001	.0010	.005
10000	.0001	.0001	.0005

TABLE 1. Relationship between Δt, maximum and truncation error

The maximum truncation in Ω_f is bounded by

$$|\tau_f| \leq \frac{\Delta t}{2}\max\Big|\frac{\partial^2 C_f}{\partial t^2}\Big| = \Delta t \max\big|x(2-x)y^2\big| = \Delta t = T_f$$

and the maximum truncation in Ω_w is bounded by

$$|\tau_w| \leq \frac{\Delta t}{2}\max\Big|\frac{\partial^2 C_w}{\partial t^2}\Big| = \Delta t \max|x(2-x)y(4-y)| = 4\Delta t = T_w.$$

So the calculated solution should be bounded by $T = T_f + T_w = 5\Delta t$. Table 1 shows how the error decreased as Δt decreased and also shows that the error is less than the maximum truncation error T. Other test cases have been considered in [4]. The experiments clearly suggested that the maximum error in the calculated solution compared to the exact solution was less than the sum of the maximum truncation errors on each domain as predicted theoretically.

Next, we demonstrate the performance of the numerical method for the coupled problem. The velocities needed for the advection-diffusion equation are obtained by solving the fluid equations as described earlier. These equations are run until the steady-state solution is reached. Then the u and v values at the (x, y) points used by the advection-diffusion equation are calculated. The diffusivity D_f and D_w is set to 1×10^{-5} as in [7]. The domain on which the chemical transport is calculated is $3 \leq x \leq 10$ and $0 \leq y \leq .31$ for Ω_f and $3 \leq x \leq 10$ and $.31 \leq y \leq .3414$ for Ω_w. The initial concentration is zero everywhere except at $\Omega_{f,up}$ and $\Omega_{w,up}$, where it is set to 100 g/cm^3. The parameter ζ is calculated by

$$\zeta = 10^{-4}(1 + |\tilde{\sigma}|) \tag{4.11}$$

where $\tilde{\sigma}$ is the stress tensor and is calculated as in [7], with

$$\tilde{\sigma} = p\tilde{I} + \nu\big[\nabla\mathbf{u} + (\nabla\mathbf{u})^T\big] \tag{4.12}$$

as in [1] where p is the pressure, $\tilde{I}$ is the 2×2 identity matrix, $\mathbf{u}$ is the velocity, and ν is the viscosity calculated on the boundary Γ. Figures 3 and 5 are the chemical concentrations on Ω_f and Ω_w, respectively, at final time. The pressure and velocities used in the chemical transport equations were the solutions to the Navier-Stokes equation and Darcy's Law. The initial concentration was set uniformly to zero and the chemical concentration on $\partial\Omega_{f,up}$ and $\partial\Omega_{w,up}$ was set to one hundred g/cm^3. Then to illustrate the role of pressure in allowing the chemical to cross the arterial wall, the pressure was set to zero and the velocities at the final time remained the same. Figures 4 and 6 suggest that significantly more chemical has entered the arterial wall in the same amount of time.
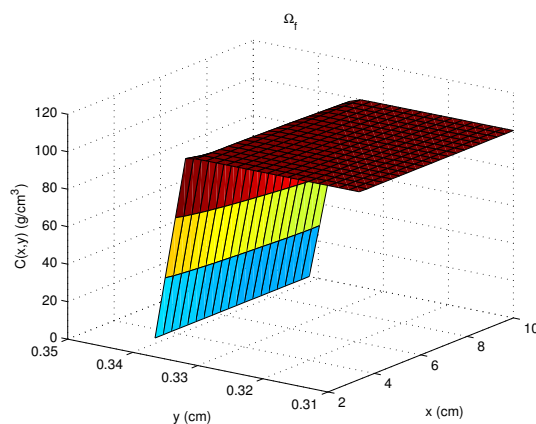
FIGURE 3. Concentration on Ω_f at final time
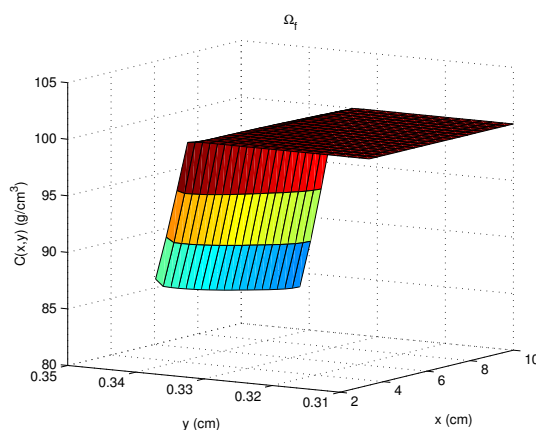
FIGURE 4. Concentration on Ω_f at final time for pressure uniformly zero.

5. CONCLUSIONS AND FUTURE DIRECTIONS

In this paper, chemical transport was coupled with Navier-Stokes and Darcy's Law and analyzed computationally. The solution methodology involved an iterative algorithm that employed the additive Schwarz method applied to two domains where the interface had mixed boundary conditions and discontinuity in the solution at the interface was allowed. A numerical software to simulate the coupled process was developed that employed the finite difference method and several numerical experiments were performed to validate the method presented herein.

The next step in modelling the chemical transport in blood flow is to allow the pressure in the vessel to move and change the thickness of the wall. We are currently studying the coupled system involving the flow and concentration equations described in this paper in the cylindrical coordinate system. To these we plan to add equations that model the visco-elastic nature of the arterial wall and study the
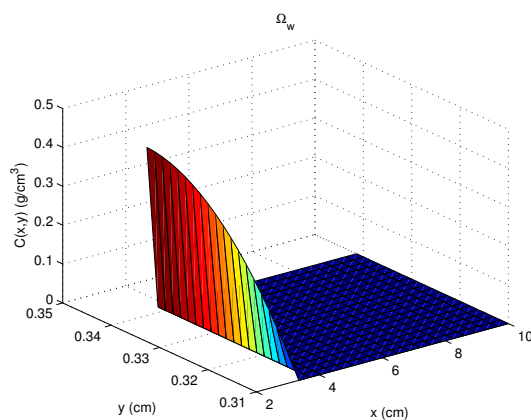
FIGURE 5. Concentration on Ω_w at final time
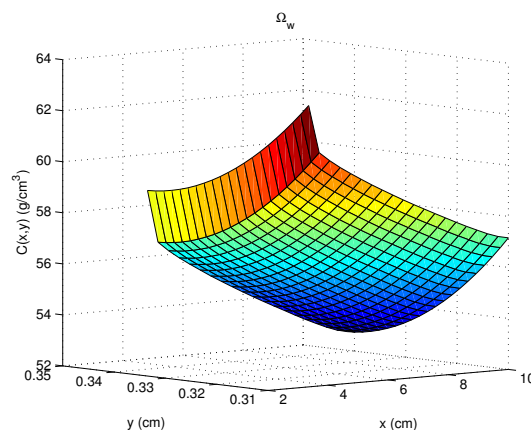
FIGURE 6. Concentration on Ω_w at final time for pressure uniformly zero.

associated fluid-structure interaction problem. This will help us to understand the effects of the moving wall on the diffusion of chemicals from the blood stream into the wall. The problem over other geometeries will also be investigated. Also, we have considered here that the chemical concentration does not change the properties of the blood and therefore does not change the velocity. We hope to consider this effect. Finally, we plan to use the model developed in conjunction with experimental data to estimate parameters. The current model provides a good insight and motivation to consider all these aspects and study the coupled fluid-structure-concentration problem which will be the focus of our forthcoming paper.

References

[1] Cheng, C. P., Parker, D., Taylor, C. A. "Quantification of Wall Shear Stress in Large Blood Vessels Using Lagrangian Interpolation Functions with Cine Phase-Contrast Magnetic Resonance Imaging," *Annals of Biomedical Engineering* 30: pp 1020-1032 (2002).

[2] Griebel, M., Dornseifer, T., Neunhoeffer, T. Numerical Simulation in Fluid Dynamics: A
    Practical Introduction. Philadelphia: Society of Industrial and Applied Mathematics, 1998.
[3] Karner, G., Perktold, K., Zehentner, H. P., Prosi, M., "Mass transport in large arteries and
    through the artery wall." In *Intra and Extracorporeal Cardiovascular Fluid Dynamics, Volume
    2-Fluid Structure Interactions*, ed. P. Verdonck and K. Pertold, 209-247. Southampton, Boston:
    WIT Press, 2000.
[4] McGee, S. M., *Computational modeling of chemical transport in flow structure interactions.*
    Doctoral disseration, Texas Tech University, Lubbock, 2007.
[5] Morton, K. W., Mayers, D. F. *Numerical Solutions of Partial Differential Equations.* Cam-
    bridge: Cambridge University Press, 1994.
[6] Press, W. H., Teukolsky, S. A., Vetterling, W. T., Flannery, B. P. *Numerical Recipes in C++.*
    Cambridge: Cambridge University Press, 2002.
[7] Quateroni, A., Veneziani, A., Zunino, P. "A domain decomposition method for advection-
    diffusion processes with application to blood solutes," *SIAM Journal of Scientific Computing*
    23: pp 1959-1980 (2002).
[8] St-Cyr, A., Gander, M. J., Thomas, S. J. "Optimized Restricted Additive Schwarz Methods."
    In *16th International Conference on Domain Decomposition.,* New York: On-line, 2004.

SHELLY MCGEE
DEPARTMENT OF MATHEMATICS, UNIVERSITY OF FINDLAY, FINDLAY, OH 45840, USA
    E-mail address: mcgee@findlay.edu

PADMANABHAN SESHAIYER
MATHEMATICAL SCIENCES, GEORGE MASON UNIVERSITY, FAIRFAX, VA 22030, USA
    E-mail address: pseshaiy@gmu.edu